Cell Calcium 80 (2019) 29–37

Contents lists available at ScienceDirect

Cell Calcium

journal homepage: www.elsevier.com/locate/ceca

Role of NAADP for calcium signaling in the salivary gland

John F. Imbery, Azwar K. Iqbal, Tanvi Desai, David R. Giovannucci*

Department of Neurosciences, University of Toledo College of Medicine and Life Sciences, 3000 Arlington Ave., Toledo, OH, 43614, United States

ARTICLE INFO

Keywords:
Calcium signaling
NAADP
Parotid acinar cells
Pancreatic acinar cells
NED19

ABSTRACT

Coordination of intracellular Ca^{2+} signaling in parotid acini is crucial for controlling the secretion of primary saliva. Previous work from our lab has demonstrated acidic-organelle Ca^{2+} release as a participant in agonist-evoked signaling dynamics of the parotid acinar cell. Furthermore, results implicated a potential role for the potent Ca^{2+} releasing second messenger NAADP in these events. The current study interrogated a direct role of NAADP for Ca^{2+} signaling in the parotid salivary gland acinar cell. Use of live-cell Ca^{2+} imaging, patch-clamp methods, and confocal microscopy revealed for the first time NAADP can evoke or enhance Ca^{2+} dynamics in parotid acini. These results were compared with pancreatic acini, a morphologically similar cell type previously shown to display NAADP-dependent Ca^{2+} signals. Findings presented here may be relevant in establishing new therapeutic targets for those suffering from xerostomia produced by hypofunctioning salivary glands.

1. Introduction

The coordination of intracellular Ca^{2+} signaling pathways in parotid acinar cells is crucial for establishing the fluid and protein components of primary saliva. While Ca^{2+} signals are largely thought to originate from ER stores, we recently revealed a novel role of acidic organelles as participants in agonist-evoked Ca^{2+} signals in parotid acinar cells [1]. Coincident β-adrenergic receptor (β-AR) activation revealed acidic organelles contributed to the Ca^{2+} signature evoked by threshold cholinergic input. In addition, in line with the role of Ca^{2+} as a co-agonist for IP_3R-mediated release and proposed "trigger-amplifier" model of nicotinic acid adenine dinucleotide phosphate (NAADP)-dependent signaling [2–5], our experiments indicated Ca^{2+} release from acidic organelles enhanced release from canonical Ca^{2+} release channels. Moreover, pharmacological and immunofluorescent approaches suggested NAADP may mediate the release of Ca^{2+} from acidic organelles. In the current study we tested whether NAADP is a Ca^{2+} mobilizing messenger in parotid acini and can initiate or contribute to fluid secretion in acini.

To investigate this hypothesis, we used enzymatically dispersed primary cultures of parotid and pancreatic acinar cells in combination with live cell Ca^{2+} imaging and electrophysiological methods. Previous work has demonstrated a repeated role for NAADP as a key second messenger in CCK-evoked Ca^{2+} signals in pancreatic acini [2,5–8]. Thus we compared our findings in parotid acinar cells with pancreatic acinar cells, a morphologically and functionally similar exocrine cell type [9–12]. We demonstrate here that the cell permeable analog NAADP-AM evoked single or repetitive Ca^{2+} transients or spikes in a subpopulation of acinar cells. Detection of spikes was enhanced when treatment with NAADP-AM was combined with the β-AR agonist isoproterenol (ISOP). Furthermore, using patch clamp methods, inclusion of NAADP in the patch pipette induced Ca^{2+}-activated Cl^- currents. These findings were compared with results from the morphologically similar, yet functionally distinct, pancreatic acinar cell. Similar to that previously reported, pancreatic acini displayed three classes of NAADP-dependent $I_{Cl(Ca)}$ signatures including spikes, a mixture of spikes, or sustained current responses. NAADP introduction into parotid acini produced only $I_{Cl(Ca)}$ spiking. These $I_{Cl(Ca)}$ spikes were modulated by ISOP and the NAADP inhibitor NED19. A final set of experiments using confocal microscopy localized NED19 intracellularly in pancreatic and parotid acinar cells, with secretory granules and endosomes being identified as binding sties in the acinar cells.

2. Materials and methods

2.1. Animal use

For all experiments, C57BL/6 male mice aged 6 months were obtained from the Jackson Laboratory (Bar Harbor, ME) or Charles River Laboratories (Wilmington, MA) and sacrificed using CO_2 asphyxiation with subsequent heart puncture. All protocols were first approved by the University of Toledo Institutional Animal Care and Use Committee and conformed to *Guide for the Care and Use of Laboratory Animals*.

* Corresponding author.
E-mail address: david.giovannucci@utoledo.edu (D.R. Giovannucci).

https://doi.org/10.1016/j.ceca.2019.03.001
Received 29 June 2018; Received in revised form 2 March 2019; Accepted 3 March 2019
Available online 04 March 2019

2.2. Isolation of parotid acinar cells

The preparation of enzymatically dissociated parotid acini was achieved as previously described [1]. Briefly, following CO_2 asphyxiation, mice underwent bilateral surgical removal of the parotid salivary glands. Glands were cleaned of fat and connective tissue, minced, and finally subjected to stepwise enzymatic Collagenase P (0.1 mg/mL) digestion at 20, 15, and 10 min intervals with intervening mechanical dissociation. Following the first incubation period, acini were triturated using a 200 μL pipette tip fitted to a serological pipette. Each subsequent trituration break made use of 1.19 mm diameter fire-polished glass pipettes. Acini were monitored periodically throughout digestion until acinar clusters were appropriately sized (˜16 acinar cells/acinus), centrifuged at 76 rcf, rinsed using BSA-free basal medium, and finally adhered to 25-mm autoclaved glass coverslips in attachment solution (BSA-free basal medium, 1% L-Glutamine, 4% Penn/Strep). Cells were allowed to settle at 37 °C before use. For patch-clamp studies using smaller clusters or individual acinar cells, acini underwent an additional 8 min digestion with 0.25% trypsin with EDTA. Pancreatic acinar cells were prepared similarly except with inclusion of 3 mg/mL trypsin inhibitor in the original digest solution.

2.3. Live-cell Ca^{2+} imaging

Ca^{2+} signals were recorded using the ratiometric fluorescent Ca^{2+} indicator Fura-2 AM as detailed previously [1,13]. Acini were loaded with Fura-2 AM and imaged on a Nikon TE2000 with DIC optics coupled to a Polychrome IV monochromator-based high-speed digital imaging system (TILL Photonics, Gräfelfing, Germany) ported to a fibre optic guide and epifluorescence condenser. Fura-2 AM was excited using dual wavelength light (340 and 380 nm) focused onto the image plane via a DM400 dichroic mirror and Nikon SuperFluor ×40 oil-immersion objective, and fluorescence obtained through a 525 ± 25 nm band-pass filter (Chroma Technologies, Brattleboro, VT). Images were collected at 1 Hz.

2.4. Electrophysiological recordings

NAADP-induced Ca^{2+}-activated Cl^- currents were recorded from individual acinar cells or small acini clusters (2–3 cells) using whole-cell patch clamping in the voltage-clamp mode (-30 to -90 mV as noted). NAADP at varying concentrations was dissolved into the intracellular recording solution that contained (mM): 140 KCl, 1.13 $MgCl_2$, 0.05 EGTA, 2 ATP and 10 HEPES, pH 7.2. Internal Ca^{2+} was buffered to a physiological level (˜130 nM) as calculated by using the online program MaxChelator (Chris Patton, Stanford). Borosilicate glass pipettes with filament (Warner Instruments, CT) were used and tips fire polished to obtain a pipette resistance 2–6 MΩ. NAADP was dialyzed into the cells following obtainment of the whole-cell configuration and subsequent $I_{Cl(Ca)}$ were isolated by using an extracellular solution that contained (mM): 140 tetraethylammonium chloride, 1 $CaCl_2$, 1.13 $MgCl_2$, 10 HEPES, 10 D-Glucose, pH 7.2. Currents were recorded at 1 kHz using an Axopatch 200 A patch-clamp amplifier (Axon Instruments, Foster City, CA, USA), ITC-16 digital interface (Instrutech, Port Washington, NY, USA), and IGOR Pro (Wavemetrics, Lake Oswego, OR, USA) and Pulse Control XOP software. The Cl- reversal potential was ˜ 0 mV.

2.5. Identification of NED19 subcellular binding location

Coverslips of isolated parotid acini were treated with LysoTracker Red (600 nM) for 30 min at 37 °C. Following LysoTracker treatment, cells were treated with NED-19 (100–200 μM) and placed in the 37 °C incubator for one hour. Cells were washed with fresh saline and subsequently imaged at room temperature using sequential scanning on a TCS SP5 laser scanning confocal microscope with a ×40 oil-immersion objective (Leica Microsystems, Bannockburn, IL) with an attached tunable Ti-sapphire multi-photon laser (Coherent, Santa Clara, CA). The excitation/emission spectrum for LysoTracker was 577/590 nm. NED19 fluorescence was acquired using the excitation/emission spectrum 389/447 nm with the multi-photon laser tuned to 770 nm.

2.6. Data analysis

Statistical analysis was performed using GraphPad Prism 3 (GraphPad Software Inc., La Jolla, CA) and values represented as the mean ± standard error with p values less than 0.05 taken as statistically significant. Unpaired t-tests were used to compare means between two unmatched groups, paired t-tests to compare means of two paired groups, and one-way ANOVA used to compare between three or more unmatched groups. $I_{Cl(Ca)}$ spikes were analyzed using IGOR Pro Software (Wavemetrics, Lake Oswego, OR, USA) where activity was detected and quantified as any peak three times above baseline noise.

2.7. Materials

All chemicals for the patch solutions, isoprenaline hydrochloride, carbamoylcholine chloride, and Collagenase P/trypsin inhibitor used in cell preparations were obtained from Sigma Aldrich (St. Louis, MO). For the live-cell Ca^{2+} imaging experiments, Fura-2AM was purchased from TefLabs (Austin, TX) and NAADP-AM from Bioquest Inc.(Sunnyvale, CA). NAADP and NED19 were acquired from Tocris (Bristol, United Kingdom). LysoTracker red and FM1-43FX were purchased from Life Technologies (Eugene, OR).

3. Results

3.1. NAADP-AM evoked Ca^{2+} dynamics

Previous work from our group indicated that Ca^{2+} release from acidic stores contributed to agonist-evoked Ca^{2+} signals in parotid acinar cells [1]. In addition, Ca^{2+} release from acidic stores was sensitive to NED19, an antagonist of NAADP-dependent signaling, and highlights a potential role for NAADP in parotid acini. In the current study, we directly demonstrate that NAADP is a Ca^{2+} mobilizing messenger in parotid acini. For initial experiments we monitored NAADP-induced Ca^{2+} signals in acini loaded with the ratiometric fluorescent Ca^{2+} indicator Fura-2 AM. Cells were perfused continuously with a bath solution containing NAADP-AM, a cell permeable version of NAADP that has previously shown to be effective in producing NAADP-dependent Ca^{2+} release in other cell types [14–16].

Over a range of concentrations (25 nM to 0.5 μM), NAADP-AM by itself produced relatively few detectable Ca^{2+} signals consisting mostly of a singular rapid and transient spike (Fig. 1A & B). This was a surprising result but extensive literature has shown signal overlap or crosstalk is extremely important for regulating parotid acinar cell output [13,17–20]. Furthermore, we have shown acidic organelle Ca^{2+} release is enhanced following elevation of cAMP in the parotid [1] and cAMP-dependent pathways are known to sensitize canonical Ca^{2+} release channels to detect localized realize [19,21]. Thus we hypothesized cAMP may be necessary to reveal NAADP-AM-dependent Ca^{2+} release. Experiments were repeated with NAADP-AM following β-AR activation with 4 μM ISOP. Our results demonstrate NAADP-AM in the presence of ISOP, or ISOP alone, largely produced similar results to NAADP-AM alone, with a few isolated spikes in most acinar clusters (Fig. 1B & D). However, a subpopulation of acini displayed an increase in the sharp and transient Ca^{2+} spikes, with 11% responding with three to four spikes and 5% responded more than five times (Fig. 1B & D). Treatment with NAADP-AM and ISOP was most effective at producing Ca^{2+} responses in the 25–200 nM range (Fig. 1C), supporting the idea of NAADP as a potent second messenger [2,3,22,23].

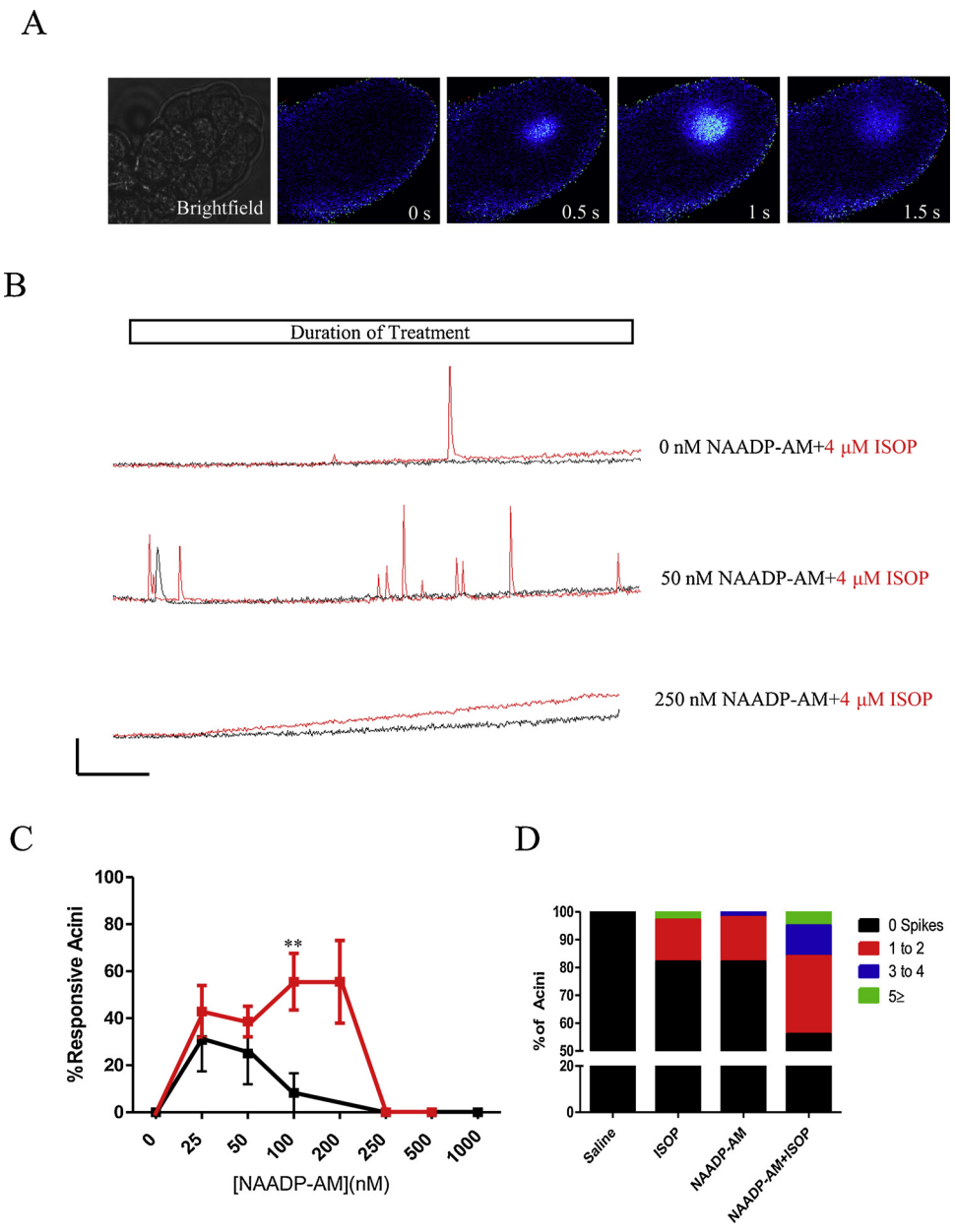

Fig. 1. NAADP-AM evoked Ca^{2+} dynamics. (A) Fura-2 AM loaded acinus with representative NAADP-AM + ISOP Ca^{2+} spike. Ca^{2+} spikes were transient and seeming to originate apically. (B) Parotid acini were perfused continuously in the presence of varying NAADP-AM concentrations, 4 μM ISOP, or NAADP-AM in combination with 4 μM ISOP (black traces are in the absence of ISOP, red traces in the presence of ISOP). NAADP-AM or ISOP alone occasionally produced isolated Ca^{2+} spikes. However, when NAADP-AM was paired with ISOP, a subpopulation of acini responded three or more times (B middle trace, D). Scale bar is 0.050 r.u. (ratio units)/50 s. (C) Concentration-response curve for NAADP-AM in the absence of ISOP (black line) and in the presence of ISOP (red line), $3 \leq n \geq 56$; $p > 0.05$ except for 100 nM NAADP versus 100 nM NAADP-AM + ISOP ($p = 0.007$). (D) A bar graph displaying distributions of Ca^{2+} spike counts. Saline ($n = 12$), ISOP alone ($n = 18$), NAADP-AM ($n = 45$) and NAADP-AM + ISOP ($n = 113$).

3.2. NAADP induced Ca^{2+}-activated Cl^- currents

Due to the variability in the responses evoked by NAADP-AM, a subsequent set of experiments used whole-cell patch clamping to introduce NAADP directly to the pancreatic and parotid acinar cells via a patch-pipette. The rationale for this set of experiments was that Ca^{2+-}activated Cl- channels have been shown to be sensitive detectors of apically localized Ca^{2+} release in pancreatic and parotid acini [11]. As a positive control to first determine if NAADP could activate Ca^{2+-}activated Cl- currents ($I_{Cl(Ca)}$)and validate our experimental paradigm, we replicated results by [2], where NAADP-activated currents were recorded in morphologically similar pancreatic acinar cells. At low nanomolar concentrations of NAADP (20–50 nM), we were able to record Ca^{2+-}activated Cl- currents. As seen previously, these currents (Fig. 2A) had distinct patterns of either spiking (43%), a combination of spiking and oscillations (50%) or sustained activation (7%). In contrast, NAADP dialysis into parotid acini produced only $I_{Cl(Ca)}$ current spiking (Fig. 2B). This was similar to earlier Ca^{2+} imaging results where NAADP-AM treatment evoked responses that were largely isolated spikes without a sustained or oscillatory signal component. Inclusion of NAADP at higher concentrations failed to evoke a significant increase in Cl- channel activation over control acinar cells (Fig. 2B). Comparison of the $I_{Cl(Ca)}$ spiking activity between acinar types revealed a trend towards a slower time to $I_{Cl(Ca)}$ spike peak amplitude in pancreatic (1.1 s ± 0.18, $n = 4$, $P = 0.051$) versus parotid (0.57 s ± 0.090, $n = 4$) acinar cells. In summary, NAADP at a low nanomolar concentrations evoked Ca^{2+}-activated Cl- activity in parotid acini with similar but distinct properties compared to NAADP-evoked responses in pancreatic acini.

3.3. Pharmacological modulation of NAADP-induced $I_{Cl(Ca)}$ activity

Having demonstrated NAADP can evoke Ca^{2+-}activated Cl- current activity in parotid acini, we tested whether the evoked release could be blocked by NED19, an antagonist of NAADP-mediated Ca^{2+} release. Acute application of NED19 induced inconsistent effects suggesting NED19 required time to load into the acinar cells, thus the experiments interrogated NAADP-dependent $I_{Cl(Ca)}$ activity following pretreatment

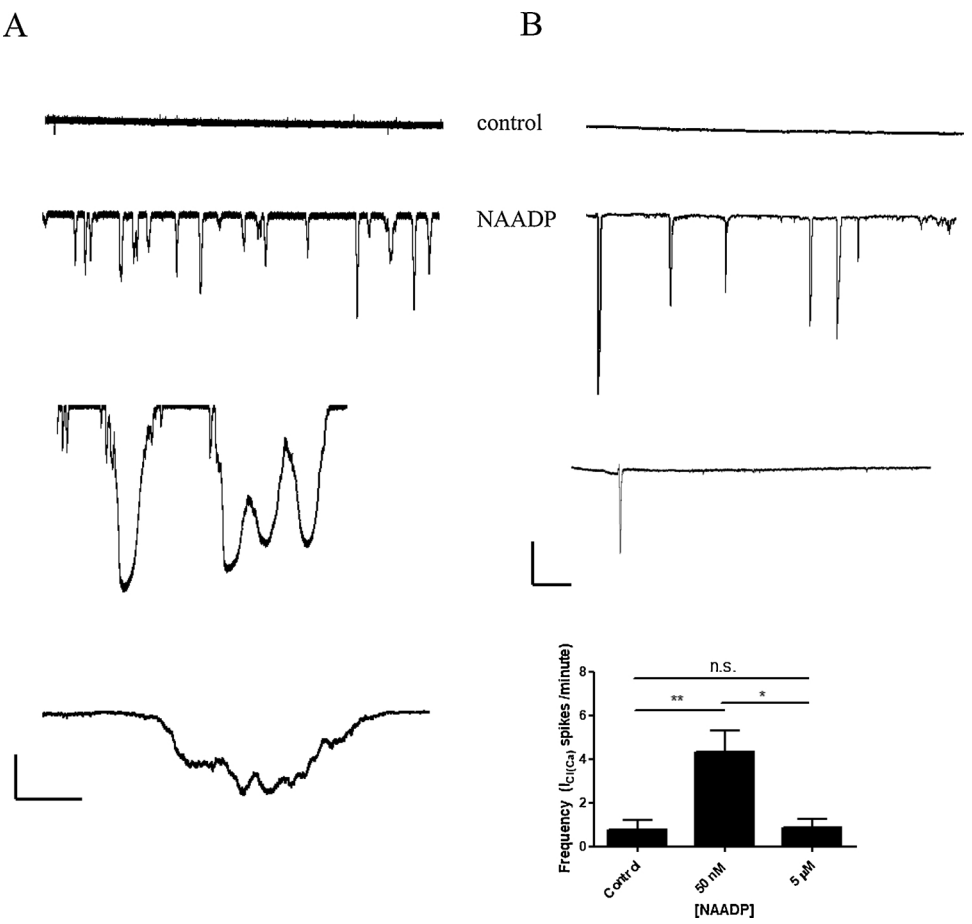

Fig. 2. NAADP induced Ca^{2+}-Activated Cl^- currents. (A) Intracellular introduction of low nanomolar [NAADP] (20–50) into pancreatic acinar cells exhibited various patterns of Ca^{2+} activated Cl^- currents including spiking (second trace), a mixture of spiking/oscillations (third trace), and a more sustained response (fourth trace) compared to patch-solution alone (first trace). Scale bar is 100 pA/50 s and cells were held at -30 mV. (B) Introduction of NAADP into parotid acinar cells resulted only in a spiking $I_{Cl(Ca)}$ signature (second trace) compared to patch-solution alone (first trace). 50 nM NAADP (second trace) produced a statistically significant increase in frequency of events (4.3 $I_{Cl(Ca)}$ spikes/minute ± 0.96, n = 7) over control parotid acinar cells (0.77 $I_{Cl(Ca)}$ spikes/minute ± 0.43, n = 6, P < 0.01) and cells introduced with 5 μM NAADP (third trace, 0.88 $I_{Cl(Ca)}$ spikes/minute ± 0.40, n = 5, P < 0.05). Scale bar is 500 pA/50 s and cells were held at -90 mV.

with NED19 and compared to control cells. With this experimental paradigm, 100 μM NED19 largely abolished NAADP activity (Fig. 3A & B). In contrast, a time-matched and vehicle control showed robust $I_{Cl(Ca)}$ activity evoked by NAADP intracellular application (data not shown). Furthermore, as a positive control, the acetylcholine receptor agonist carbachol (CCh) was used (5 μM) to evoke $I_{Cl(Ca)}$ responses in NED19 treated acini to indicate Cl- channels were still responsive. Although NED19 treated cells were shown to respond following CCh application (Fig. 3A), the cells had a statistically significant reduction in peak CCh-evoked $I_{Cl(Ca)}$ (485.9 pA ± 222.8, n = 6, P = 0.035) in comparison to untreated, NAADP-introduced acinar cells (1393 pA ± 286.0, n = 4). This result was similar to observed NED19-dependent reduction in CCh-induced Ca^{2+} signals seen previously in our lab [1].

In the pancreatic acinar cell, there are agonist-specific elevations of second messengers. Muscarinic activation is preferentially coupled to cADPR and IP_3 production, while physiological concentrations of CCK are coupled to cADPR and NAADP synthesis [24]. Moreover, these pathways have been shown to converge to shape the generation of Ca^{2+} signals and $I_{Cl(Ca)}$ activity in the pancreatic acinar cell [6,7]. We next assessed whether NAADP-dependent $I_{Cl(Ca)}$ activity can similarly integrate with canonically activated intracellular pathways to modulate the $I_{Cl(Ca)}$ activity signature. To test this hypothesis, we assessed the role of a cAMP elevator on NAADP-evoked $I_{Cl(Ca)}$ activity by activation of the β-AR. Treatment with the β-AR agonist ISOP alone resulted in an occasional isolated $I_{Cl(Ca)}$ spike that was not significantly different from control (Fig. 3D). However, when ISOP was applied following intracellular application of NAADP, we observed an increase in spike frequency as well as an occasional sustained and often oscillatory $I_{Cl(Ca)}$ response (FIC 3C & 3D). These results were consistent with the observation NAADP-AM treatment in combination with ISOP caused an increase in NAADP-AM spikes in a subpopulation of acini and with data from our lab and others where second messenger pathways integrate to modify agonist-evoked responses in acinar cells [1,6,7,13]. Additional evidence using the adenylate cyclase agonist forskolin revealed a similar enhancement (Fig. 3E) of the NAADP $I_{Cl(Ca)}$ suggesting cAMP is a key second messenger regulating this signal cross talk.

3.4. Subcellular localization of NED19 uptake

To further clarify a role for NAADP in the parotid acini, we sought to identify potential subcellular binding locations for NAADP. Previous work from our lab indicated secretory granules were the dominant subcellular site for acidic store Ca^{2+} release and thus a likely site for NAADP binding. To localize potential NAADP binding sites we used fluorescence imaging following treatment of acini with NED19. NED19 was identified based on overlap of its three dimensional configuration and electrostatic charge with NAADP as originally ascertained via virtual screening of an electronic database containing commercially available compounds [25]. Using sea urchin egg homogenates as a bioassay, NED19 was found to be the most potent inhibitor of NAADP-dependent signaling and because NED19 was a tryptophan derivative, its inherent fluorescence could be exploited to reveal its subcellular location following incubation in NAADP responsive tissues [25]. Indeed, NED19 has been used to identify potential NAADP binding sites in a variety of systems including sea urchin eggs [25], astrocytes [15], and murine naïve T-cells [26].

In this set of experiments, we treated pancreatic acini with LysoTracker red, a live-cell fluorescent dye that preferentially accumulates in intracellular compartments with low pH, followed by incubation with NED19 and subsequent imaging via confocal microscopy. Fig. 4A-D showed that NED19 partially localized with acidic organelles in pancreatic acini. Based on a previous study, these organelles were

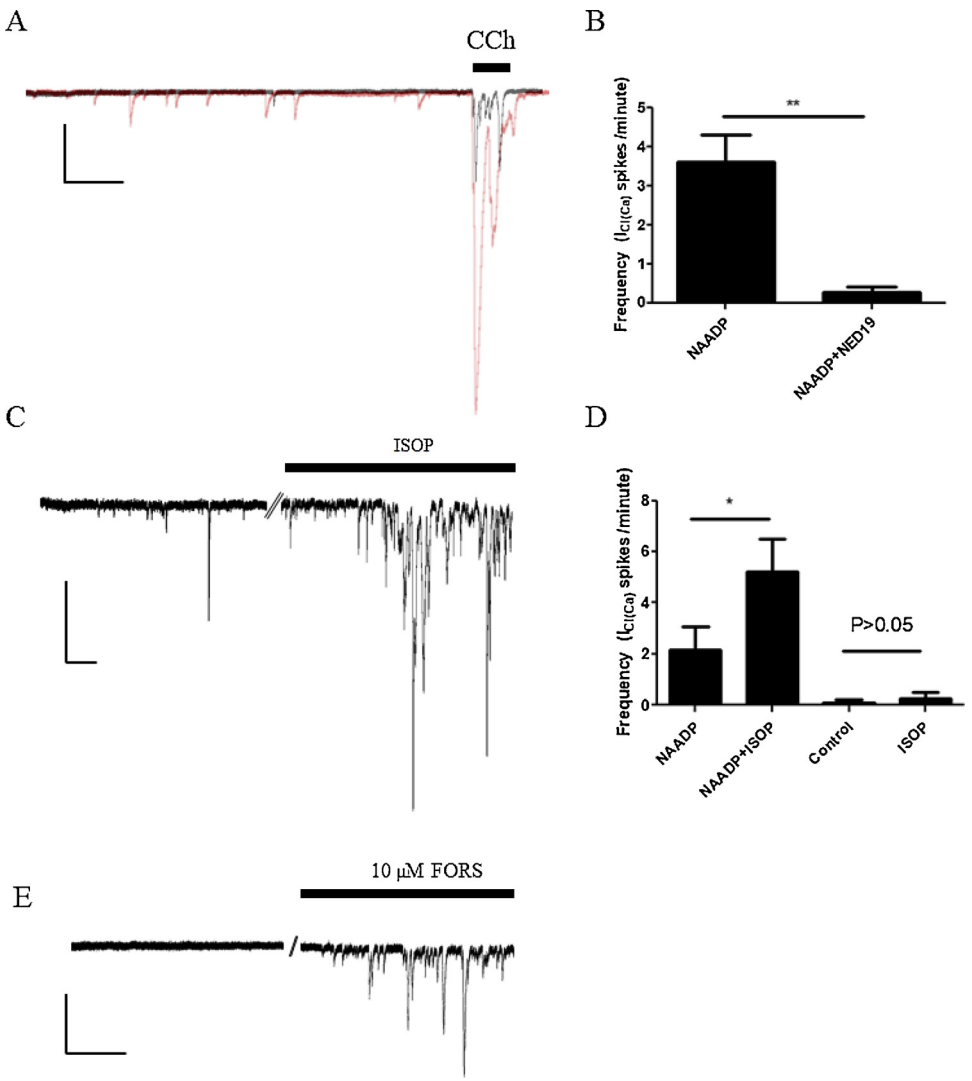

Fig. 3. Pharmacological modulation of NAADP-induced $I_{Cl(Ca)}$ activity. (A) Parotid acinar cells were pretreated with NED19 prior to intracellular introduction of NAADP. Red trace represents NAADP alone, black trace represents NAADP + NED19 pretreatment. Scale bar is 100 pA/25 s. (B) Pretreatment with NED19 reduced the frequency of NAADP-dependent $I_{Cl(Ca)}$ (0.28 $I_{Cl(Ca)}$ spikes/minute ± 0.13, $n = 7$, $P < 0.01$) in comparison to cells without NED19 pretreatment (3.6 $I_{Cl(Ca)}$ spikes/minute ± 0.70, $n = 7$). Scale bar is 200 pA/25 s. (C) ISOP perfusion was paired with cells currently responding to NAADP. (D) The frequency of NAADP-dependent $I_{Cl(Ca)}$ (2.1 $I_{Cl(Ca)}$ spikes/minute ± 0.88, $n = 7$) could be enhanced to statistical significance in the presence of ISOP (5.2 $I_{Cl(Ca)}$ spikes/minute ± 1.3, $n = 7$, $P < 0.05$). ISOP treatment alone (0.27 $I_{Cl(Ca)}$ spikes/minute ± 0.24, $n = 6$) did not produce a statistically significant increase in the frequency of events in comparison to controls ($I_{Cl(Ca)}$ spikes/minute ± 0.089, $n = 9$, $P > 0.05$). (E) There was an observable enhancement in $I_{Cl(Ca)}$ following extracellular perfusion of 10 μM FORS in 2 out of 3 parotid acinar cells not originally responding to intracellular application of a low nanomolar [NAADP]. Cells were held at -50 mV. The scale bar is 100 pA/10 s. Recordings were obtained at a holding potential of -50 mV.

likely the secretory granules that are thought to be the site of NAADP-evoked Ca^{2+} release in this cell type [5], although we cannot rule out the possibility of another acidic organelle population also being labeled. In contrast, when parotid acinar cells were imaged following NED19 treatment, NED19 fluorescence was found to localize only in close proximity with acidic organelles that were largely distributed along the periphery of the region containing the smaller secretory granules (Fig. 4E–H). One possibility was that NED19 co-localized to a late endosomal compartment. To test this possibility, we used the membrane probe FM1-43. FM1-43 is weakly fluorescent in aqueous environments but increases its fluorescent yield upon incorporation into the plasma membrane and thus can be used as marker for endosomes being formed as a result of membrane retrieval. Acini were unstimulated and stained with FM1-43 (10 μM) in combination with NED19 for one hour and imaged directly following incubation. As these acini were unstimulated, intracellular punctate labeling by FM1-43 is a reflection of constitutive endocytosis. As hypothesized, these endosomes and NED19 fluorescence overlapped or were in close proximity (Fig. 4C). Similar results were observed when Texas-Red dye, in place of FM1-43, was used as a fluid phase tracer. These surprising results suggested that NED19 binding, and by inference NAADP binding, may be localized to a late endosomal compartment rather than on secretory granules in the parotid acini.

In conclusion, pharmacological and patch-clamp data highlight a novel NAADP signaling pathway in parotid acinar cells. This extends findings from the literature where NAADP has been shown to be an important second messenger in a variety of cell types, including the morphologically similar pancreatic acinar cell, and suggests NAADP may be an important regulator of parotid salivary function. A model of NAADP's actions in parotid acinar cells can be seen in Fig. 5.

4. Discussion

The first mammalian cell-type where NAADP was shown to induce Ca^{2+} release was the pancreatic acinar cell [2]. Here, the current study revealed for the first time a role for NAADP in acinar cells of the parotid salivary gland. The following discussion will compare between NAADP-dependent signaling in pancreatic acinar cells versus our findings in parotid acinar cells with respect to the relevance of Ca^{2+}-induced Ca^{2+} release (CICR), NAADP binding sites and synthesis, in addition to signal crosstalk and parotid salivary gland acinar function.

4.1. Calcium induced calcium release

In pancreatic acinar cells, NAADP responses could be recorded in the absence of extracellular Ca^{2+} demonstrating NAADP evoked Ca^{2+} signals from internal stores [2]. Additionally, NAADP Ca^{2+} signatures where sensitive to IP_3 and cADPR inhibitors with neither messenger being sensitive to inhibitory concentrations of NAADP [2]. These observations led to the "trigger-amplify" model of NAADP-dependent

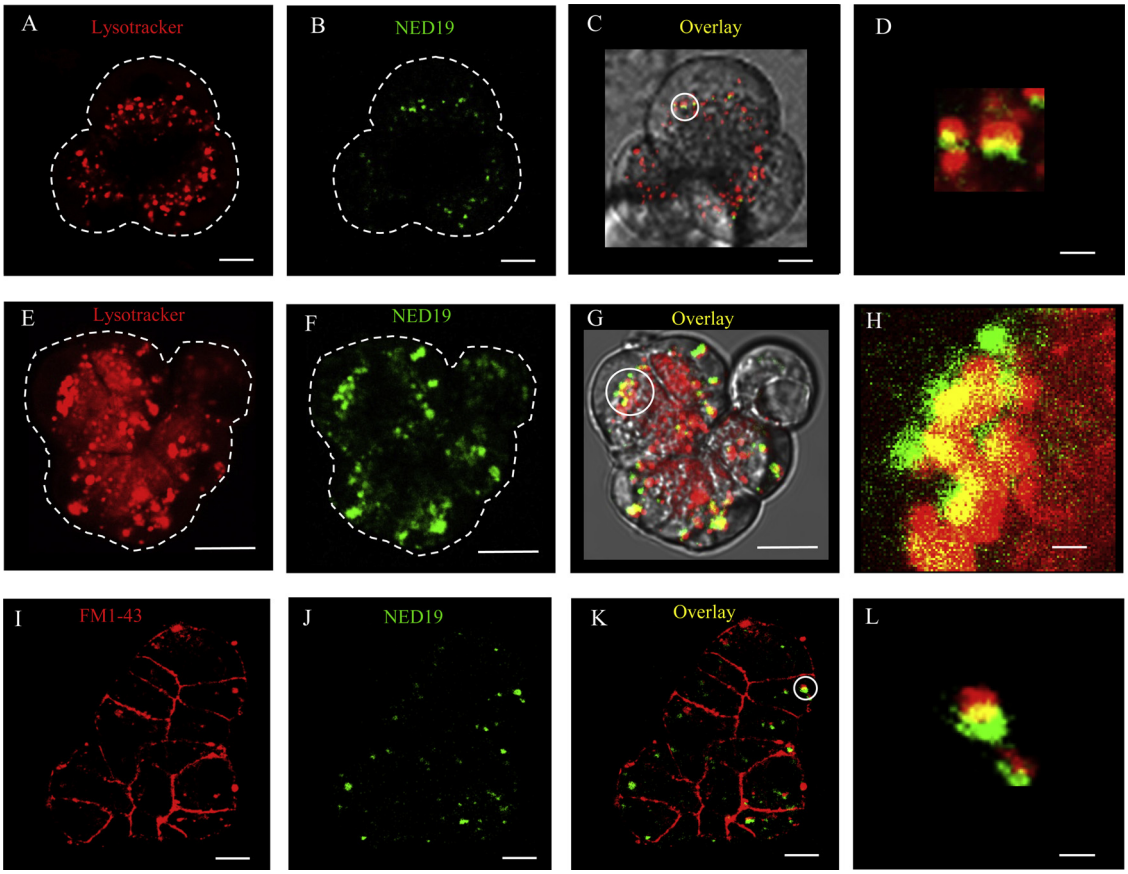

Fig. 4. Subcellular localization of NED19 fluorescence. (A–D) NED19 fluorescence (green) was largely apically distributed and colocalized with a subpopulation of acidic organelles (red) in a pancreatic acinus. The average number of organelles with overlapping NED19-Lysotracker fluorescence signals in a pancreatic acinar cell was 8.6 puncta (n = 7). (E–H) In the parotid acinus, NED19 fluorescence (green) overlapped with acidic organelles (red) largely located outside the apical granule-containing region. The average number of organelles labeled with both NED19 and Lysotracker fluorescence in a parotid acinar cell was 2.8 (n = 8). (I–L) In a parotid acinus, labeling with the membrane probe FM1-43 (red) suggested that Lysotracker-labeled acidic organelles were likely endosomes. As shown, FM1-43 labeled organelles often overlapped with NED19 fluorescence (green). White circles indicate NED19-labeled acidic organelles (C, G) or FM1-43 puncta (K). Scale bars are 8 μm for large images and 600 nm for enlarged areas indicated by circled regions, respectively. Each experiment was replicated at least three times.

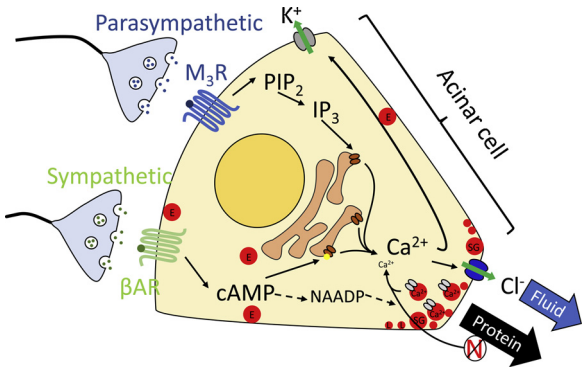

Fig. 5. Model of NAADP signaling in parotid acinar cells. Acidic organelles, red, consist of SG (secretory granules), L (lysosomes), and endosomes (E) distributed along apicolateral boarders. Parasympathetic activation leads to IP_3-dependent liberation of Ca^{2+} from ER stores. Sympathetic input elevates cAMP, which can phosphorylate IP_3 receptors (yellow circle) and likely recruits a NAADP-dependent pathway releasing Ca^{2+} from secretory granules [1] and/or perhaps endosomes. We hypothesize localized acidic organelle Ca^{2+} release by NAADP triggers release from proximally located ER Ca^{2+} channels via CICR and can be enhanced with coincident application of ISOP. NAADP generates Ca^{2+}-dependent Cl^- activity that may be sufficient for initiating fluid secretion although acidic organelle Ca^{2+} is not necessary for protein release.

signaling [2], where localized release of Ca^{2+} by NAADP from acidic organelles recruited activation of canonical ER Ca^{2+} channels via CICR. The importance of localized Ca^{2+} for NAADP signaling in pancreatic acinar cells was confirmed by [5] and the CICR model of acidic organelle Ca^{2+} signaling has been a consistent theme in the field [2–46,22,24]. For parotid acinar cells, NAADP-AM Ca^{2+} signals appeared to originate apically, indicative of release. This is consistent with previous work from our lab where acidic organelles contributed to ER-dependent Ca^{2+} release [1] and likely indicated localized Ca^{2+} release from acidic organelles by NAADP triggers release from the ER via CICR in parotid acinar cells.

Interestingly, NAADP evoked responses only in a subpopulation of parotid acinar cells. This is similar to that observed in pancreatic acinar cells where ~75% of cells responded to NAADP [2]. One possibility is that prep-to-prep variability produced by enzymatic digestion of acini accounted for this observation. On the other hand, it is possible only a subpopulation of acinar cells are equipped with the appropriate machinery necessary for NAADP Ca^{2+} release. This latter assertion is consistent with the fact not all acinar cells responded within an acinus during NAADP-AM live-cell Ca^{2+} imaging.

4.2. NAADP binding sites

The NAADP-targeted Ca^{2+} release channel has remained elusive, with endolysosomal TRP mucolipin channels [27,28] and the ryanodine receptor [29] implicated in various systems, although the most

substantial evidences supports the two-pore channel [30–32] as the NAADP targeted receptor. Regardless of the exact identity of the channel, a consensus exists that NAADP releases Ca^{2+} from the apical granular region in pancreatic acinar cells [5–7] and is further supported by our localization of NED19 fluorescence to apical acidic organelles in this cell. Results from our lab also suggested apically localized secretory granules in the parotid acinar cell as the site for NAADP actions [1] although NED19 fluorescence was situated near basal late endosomes. The disparity in these results are not immediately clear. It could represent differences in NED19 uptake or entry between the acinar types. Furthermore, the low molecular weight of NED19 makes it unlikely we could detect its fluorescent emissions if only a small amount was bound to the secretory granules. Endosomes have been implicated as a potential site of NAADP-dependent Ca^{2+} release [33] and contain endolysosomal channels activated by NAADP [27,28,33], however endosomal localization to basal regions in the parotid is in contrast to evidence that Ca^{2+} release is triggered apically [11,34,35]. Ultimately, additional research into endosomal and Ca^{2+} release pathways could be particularly revealing, especially with increasing evidence linking the endolysosomal system to disease pathophysiology [36,37].

4.3. NAADP synthesis

Prevailing arguments propose NAADP synthesis occurs through a base-exchange reaction with the nicotinamide moiety of NADP exchanged for nicotinic acidic. This occurs in enzymes possessing ADP-ribosyl cyclase activity such as CD38 and CD157 [38–40] within an acidic environment. Indeed, CD38 was shown to localize near the apical membrane and with an early endosomal marker in the pancreatic acinar cell, suggesting NAADP may be synthesized in an internal acidic environment [39]. Additionally, CCK-dependent NAADP synthesis and signaling were abolished in pancreatic acinar cells derived from CD38 knockout animals [39]. Although a role for CD38 was not tested in the current study, future experiments linking receptor activation to NAADP synthesis and degradation will be important in solidifying its role as a second messenger in parotid acinar cells.

4.4. Signal crosstalk

Signal crosstalk is believed to be an important factor coordinating the functional output of parotid acinar cells [13,17–20]. In fact, signal crosstalk occurring during coincident activation of cholinergic, adrenergic driven pathways in parotid acinar cells leads to a synergistic enhancement of primary saliva secretion. Although the upstream activators of the NAADP signaling pathway needs further elucidation, we demonstrate a novel interaction between NAADP-dependent $I_{Cl(Ca)}$ activity and activation of canonical β-AR driven pathways via ISOP. Activation of β-ARs is thought to largely elevate cAMP in parotid acinar cells [41–43]. In addition, cAMP-dependent phosphorylation of IP_3Rs receptors sensitizes these channels for detecting localized release of Ca^{2+} [19]. As such an enhancement of the NAADP-dependent $I_{Cl(Ca)}$ signature is likely due to the phosphorylation state of canonical ER Ca^{2+} channels and their enhanced ability to detect localized release of Ca^{2+}. This could represent a potential convergence point in the parotid acinar cell regulating the construction of a Ca^{2+} signal and represent an additional mechanism underlying cholinergic, adrenergic signal crosstalk. Ultimately, signal crosstalk arising from NAADP-dependent signaling could have potentially significant implications for regulating the biological output of parotid acinar cells.

4.5. Physiological role

Intracellular Ca^{2+} signals can be generated by agonist-induced increases in Ca^{2+}-mobilizing second messengers including IP_3, cyclic ADP-ribose and NAADP. Of these, NAADP was shown to be the most potent Ca^{2+} releasing messenger with maximal potency occurring in the low nanomolar range. Furthermore, NAADP was shown to evoke Ca^{2+} release from intracellular acidic organellular reserves [44] that include lysosomes, endosomes, and secretory granules [33,45]. NAADP-mediated Ca^{2+} release from these organelles has since been demonstrated to modulate processes including glucose induced insulin release from pancreatic beta cells [3], T-lymphocyte activation [46], neurite outgrowth [47], and even quite recently neuronal plasticity [48].

Ca^{2+}-activated Cl^- currents have been used repeatedly as a bioassay for assessing Ca^{2+} release in acinar cells [2,6,11,49–51]. To our knowledge, results presented here are the first demonstration of NAADP Ca^{2+}-activated Cl^- currents in parotid acinar cells. That differences existed in NAADP-dependent $I_{Cl(Ca)}$ between the two acinar cell types may not be particularly surprising, as results comparing $I_{Cl(Ca)}$ activity following uncaging of IP_3 and Ca^{2+} revealed diverging characteristics [11]. NAADP-dependent $I_{Cl(Ca)}$ activity could be attributable to differences in NAADP receptor subcellular density, acidic organellular populations, the total Ca^{2+} stored in acidic organelles, or Ca^{2+} buffering capacity between the two acinar cells. However, the NAADP-dependent $I_{Cl(Ca)}$ signatures may also reflect different physiological roles for pancreatic and parotid acinar cells. Pancreatic acinar cells are responsible for packaging and secreting proenzymes necessary for digestion, a relatively slow process that may be reflected by the temporally slower oscillatory and sustained NAADP-dependent $I_{Cl(Ca)}$ activity. Accordingly, NAADP responses are evoked by the CCK in the pancreas [2,24], a hormone that can likely remain elevated for minutes following secretion. In contrast, NAADP-dependent $I_{Cl(Ca)}$ spikes might encode the rapid mobilization of fluid and electrolyte salivary secretion from parotid acinar cells initiated by fast-acting neurotransmitters. Further investigation into the contributions to and physiological consequences of NAADP $I_{Cl(Ca)}$ signatures is warranted.

It is thought that Ca^{2+}-dependent Cl^- channel activation is critical for fluid production [52–55] and suggests NAADP has a role in secreting a component of primary saliva. Thus NAADP may serve as a potential therapeutic target for those suffering from xerostomia, or dry mouth, resulting from hypofunctioning salivary glands produced by autoimmune disorders like Sjögren's Syndrome. Indeed, canonical IP_3-dependent Ca^{2+} release pathways are thought to be altered in Sjögren's due to autoantibodies targeting the muscarinic receptor [56–58] and deficits in IP_3Rs themselves [59]. Whether release of Ca^{2+} via NAADP could be achieved to offset these signaling deficits by sensitizing remaining Ca^{2+} channels to restore or augment the secretory function of parotid acinar cells and offer therapeutic relief from dry mouth may warrant further investigation.

Funding

This work was funded by National Institute of Dental and Craniofacial Research grant DE-023418.

Author contributions

J.F.I designed and performed experiments, analyzed the data and wrote and edited the manuscript. A.K.I and T.D. acquired and analyzed the data. D.G. conceived and directed the research, reviewed the data, and edited the manuscript.

Conflict of interest

None.

Acknowledgements

The authors thank Dr. Andrea Kalinoski in the Advanced Microscopy and Imaging Core at the University of Toledo Health Science Campus for assistance with the multi-photon microscopy.

Appendix A. Supplementary data

Supplementary material related to this article can be found, in the online version, at doi:https://doi.org/10.1016/j.ceca.2019.03.001.

References

[1] J.F. Imbery, S. Bhattacharya, S. Khuder, A. Weiss, P. Goswamee, A.K. Iqbal, D.R. Giovannucci, cAMP-dependent recruitment of acidic organelles for Ca2+ signaling in the salivary gland, Am. J. Physiol. Cell Physiol. 311 (2016) C697–C709.

[2] J.M. Cancela, G.C. Churchill, A. Galione, Coordination of agonist-induced Ca2+-signalling patterns by NAADP in pancreatic acinar cells, Nature 398 (1999) 74–76.

[3] R. Masgrau, G.C. Churchill, A.J. Morgan, S.J. Ashcroft, A. Galione, NAADP: a new second messenger for glucose-induced Ca2+ responses in clonal pancreatic beta cells, Curr. Biol. 13 (2003) 247–251.

[4] N.P. Kinnear, F.X. Boittin, J.M. Thomas, A. Galione, A.M. Evans, Lysosome-sarcoplasmic reticulum junctions. A trigger zone for calcium signaling by nicotinic acid adenine dinucleotide phosphate and endothelin-1, J. Biol. Chem. 279 (2004) 54319–54326.

[5] J.V. Gerasimenko, M. Sherwood, A.V. Tepikin, O.H. Petersen, O.V. Gerasimenko, NAADP, cADPR and IP3 all release Ca2+ from the endoplasmic reticulum and an acidic store in the secretory granule area, J. Cell. Sci. 119 (2006) 226–238.

[6] J.M. Cancela, O.V. Gerasimenko, J.V. Gerasimenko, A.V. Tepikin, O.H. Petersen, Two different but converging messenger pathways to intracellular Ca(2+) release: the roles of nicotinic acid adenine dinucleotide phosphate, cyclic ADP-ribose and inositol trisphosphate, EMBO J. 19 (2000) 2549–2557.

[7] J.M. Cancela, F. Van Coppenolle, A. Galione, A.V. Tepikin, O.H. Petersen, Transformation of local Ca2+ spikes to global Ca2+ transients: the combinatorial roles of multiple Ca2+ releasing messengers, EMBO J. 21 (2002) 909–919.

[8] J.V. Gerasimenko, R.M. Charlesworth, M.W. Sherwood, P.E. Ferdek, K. Mikoshiba, J. Parrington, O.H. Petersen, O.V. Gerasimenko, Both RyRs and TPCs are required for NAADP-induced intracellular Ca(2)(+) release, Cell Calcium 58 (2015) 237–245.

[9] M.G. Lee, X. Xu, W. Zeng, J. Diaz, T.H. Kuo, F. Wuytack, L. Racymaekers, S. Muallem, Polarized expression of Ca2+ pumps in pancreatic and salivary gland cells. Role in initiation and propagation of [Ca2+]i waves, J. Biol. Chem. 272 (1997) 15771–15776.

[10] M.G. Lee, X. Xu, W. Zeng, J. Diaz, R.J. Wojcikiewicz, T.H. Kuo, F. Wuytack, L. Racymaekers, S. Muallem, Polarized expression of Ca2+ channels in pancreatic and salivary gland cells. Correlation with initiation and propagation of [Ca2+]i waves, J. Biol. Chem. 272 (1997) 15765–15770.

[11] D.R. Giovannucci, J.I. Bruce, S.V. Straub, J. Arreola, J. Sneyd, T.J. Shuttleworth, D.I. Yule, Cytosolic Ca(2+) and Ca(2+)-activated Cl(-) current dynamics: insights from two functionally distinct mouse exocrine cells, J. Physiol. 540 (2002) 469–484.

[12] O.H. Petersen, A.V. Tepikin, Polarized calcium signaling in exocrine gland cells, Annu. Rev. Physiol. 70 (2008) 273–299.

[13] S. Bhattacharya, J.F. Imbery, P.T. Ampem, D.R. Giovannucci, Crosstalk between purinergic receptors and canonical signaling pathways in the mouse salivary gland, Cell Calcium (2015).

[14] R. Parkesh, A.M. Lewis, P.K. Aley, A. Arredouani, S. Rossi, R. Tavares, S.R. Vasudevan, D. Rosen, A. Galione, J. Dowden, G.C. Churchill, Cell-permeant NAADP: a novel chemical tool enabling the study of Ca2+ signalling in intact cells, Cell Calcium 43 (2008) 531–538.

[15] M. Barcelo-Torns, A.M. Lewis, A. Gubern, D. Barneda, D. Bloor-Young, F. Picatoste, G.C. Churchill, E. Claro, R. Masgrau, NAADP mediates ATP-induced Ca2+ signals in astrocytes, FEBS Lett. 585 (2011) 2300–2306.

[16] A. Galione, K.T. Chuang, T.M. Funnell, L.C. Davis, A.J. Morgan, M. Ruas, J. Parrington, G.C. Churchill, Synthesis of NAADP-AM as a membrane-permeant NAADP analog, Cold Spring Harb. Protoc. 2014 (2014) pdb prot076927.

[17] B. Asking, Sympathetic stimulation of amylase secretion during a parasympathetic background activity in the rat parotid gland, Acta Physiol. Scand. 124 (1985) 535–542.

[18] N. Emmelin, Nerve interactions in salivary glands, J. Dent. Res. 66 (1987) 509–517.

[19] J.I. Bruce, T.J. Shuttleworth, D.R. Giovannucci, D.I. Yule, Phosphorylation of inositol 1,4,5-trisphosphate receptors in parotid acinar cells. A mechanism for the synergistic effects of cAMP on Ca2+ signaling, J. Biol. Chem. 277 (2002) 1340–1348.

[20] G.B. Proctor, G.H. Carpenter, Regulation of salivary gland function by autonomic nerves, Autonomic neuroscience: basic & clinical 133 (2007) 3–18.

[21] J.S. McKinney, M.S. Desole, R.P. Rubin, Convergence of cAMP and phosphoinositide pathways during rat parotid secretion, Am. J. Physiol. 257 (1989) C651–657.

[22] A. Macgregor, M. Yamasaki, S. Rakovic, L. Sanders, R. Parkesh, G.C. Churchill, A. Galione, D.A. Terrar, NAADP controls cross-talk between distinct Ca2+ stores in the heart, J. Biol. Chem. 282 (2007) 15302–15311.

[23] A.J. Morgan, A. Galione, Investigating cADPR and NAADP in intact and broken cell preparations, Methods 46 (2008) 194–203.

[24] M. Yamasaki, J.M. Thomas, G.C. Churchill, C. Garnham, A.M. Lewis, J.M. Cancela, S. Patel, A. Galione, Role of NAADP and cADPR in the induction and maintenance of agonist-evoked Ca2+ spiking in mouse pancreatic acinar cells, Curr. Biol. 15 (2005) 874–878.

[25] E. Naylor, A. Arredouani, S.R. Vasudevan, A.M. Lewis, R. Parkesh, A. Mizote, D. Rosen, J.M. Thomas, M. Izumi, A. Ganesan, A. Galione, G.C. Churchill, Identification of a chemical probe for NAADP by virtual screening, Nat. Chem. Biol. 5 (2009) 220–226.

[26] R.A. Ali, C. Camick, K. Wiles, T.F. Walseth, J.T. Slama, S. Bhattacharya, D.R. Giovannucci, K.A. Wall, Nicotinic acid adenine dinucleotide phosphate plays a critical role in naive and effector murine t cells but not natural regulatory t cells, J. Biol. Chem. 291 (2016) 4503–4522.

[27] F. Zhang, P.L. Li, Reconstitution and characterization of a nicotinic acid adenine dinucleotide phosphate (NAADP)-sensitive Ca2+ release channel from liver lysosomes of rats, J. Biol. Chem. 282 (2007) 25259–25269.

[28] F. Zhang, M. Xu, W.Q. Han, P.L. Li, Reconstitution of lysosomal NAADP-TRP-ML1 signaling pathway and its function in TRP-ML1(-/-) cells, Am. J. Physiol. Cell Physiol. 301 (2011) C421–430.

[29] A. Mojzisova, O. Krizanova, L. Zacikova, V. Kominkova, K. Ondrias, Effect of nicotinic acid adenine dinucleotide phosphate on ryanodine calcium release channel in heart, Pflugers Arch. 441 (2001) 674–677.

[30] P.J. Calcraft, M. Ruas, Z. Pan, X. Cheng, A. Arredouani, X. Hao, J. Tang, K. Rietdorf, L. Teboul, K.T. Chuang, P. Lin, R. Xiao, C. Wang, Y. Zhu, Y. Lin, C.N. Wyatt, J. Parrington, J. Ma, A.M. Evans, A. Galione, M.X. Zhu, NAADP mobilizes calcium from acidic organelles through two-pore channels, Nature 459 (2009) 596–600.

[31] S. Yamaguchi, A. Jha, Q. Li, A.A. Soyombo, G.D. Dickinson, D. Churamani, E. Brailoiu, S. Patel, S. Muallem, Transient receptor potential mucolipin 1 (TRPML1) and two-pore channels are functionally independent organellar ion channels, J. Biol. Chem. 286 (2011) 22934–22942.

[32] M. Ruas, L.C. Davis, C.C. Chen, A.J. Morgan, K.T. Chuang, T.F. Walseth, C. Grimm, C. Garnham, T. Powell, N. Platt, F.M. Platt, M. Biel, C. Wahl-Schott, J. Parrington, A. Galione, Expression of Ca(2)(+)-permeable two-pore channels rescues NAADP signalling in TPC-deficient cells, EMBO J. 34 (2015) 1743–1758.

[33] S. Patel, R. Docampo, Acidic calcium stores open for business: expanding the potential for intracellular Ca2+ signaling, Trends Cell Biol. 20 (2010) 277–286.

[34] Y. Tojyo, A. Tanimura, Y. Matsumoto, Imaging of intracellular Ca2+ waves induced by muscarinic receptor stimulation in rat parotid acinar cells, Cell Calcium 22 (1997) 455–462.

[35] H. Takemura, S. Yamashina, A. Segawa, Millisecond analyses of Ca2+ initiation sites evoked by muscarinic receptor stimulation in exocrine acinar cells, Biochem. Biophys. Res. Commun. 259 (1999) 656–660.

[36] E. Lloyd-Evans, A.J. Morgan, X. He, D.A. Smith, E. Elliot-Smith, D.J. Sillence, G.C. Churchill, E.H. Schuchman, A. Galione, F.M. Platt, Niemann-Pick disease type C1 is a sphingosine storage disease that causes deregulation of lysosomal calcium, Nat. Med. 14 (2008) 1247–1255.

[37] Y.B. Hu, E.B. Dammer, R.J. Ren, G. Wang, The endosomal-lysosomal system: from acidification and cargo sorting to neurodegeneration, Transl. Neurodegener. 4 (2015) 18.

[38] E.N. Chini, C.C. Chini, I. Kato, S. Takasawa, H. Okamoto, CD38 is the major enzyme responsible for synthesis of nicotinic acid-adenine dinucleotide phosphate in mammalian tissues, Biochem. J. 362 (2002) 125–130.

[39] F. Cosker, N. Cheviron, M. Yamasaki, A. Menteyne, F.E. Lund, M.J. Moutin, A. Galione, J.M. Cancela, The ecto-enzyme CD38 is a nicotinic acid adenine dinucleotide phosphate (NAADP) synthase that couples receptor activation to Ca2+ mobilization from lysosomes in pancreatic acinar cells, J. Biol. Chem. 285 (2010) 38251–38259.

[40] S.Y. Rah, M. Mushtaq, T.S. Nam, S.H. Kim, U.H. Kim, Generation of cyclic ADP-ribose and nicotinic acid adenine dinucleotide phosphate by CD38 for Ca2+ signaling in interleukin-8-treated lymphokine-activated killer cells, J. Biol. Chem. 285 (2010) 21877–21887.

[41] J. Fujita-Yoshigaki, Divergence and convergence in regulated exocytosis: the characteristics of cAMP-dependent enzyme secretion of parotid salivary acinar cells, Cell. Signal. 10 (1998) 371–375.

[42] T. Takuma, T. Ichida, Does cyclic AMP mobilize Ca2+ for amylase secretion from rat parotid cells? Biochim. Biophys. Acta 887 (1986) 113–117.

[43] K. Yoshimura, J. Fujita-Yoshigaki, M. Murakami, A. Segawa, Cyclic AMP has distinct effects from Ca(2+) in evoking priming and fusion/exocytosis in parotid amylase secretion, Pflugers Arch. 444 (2002) 586–596.

[44] G.C. Churchill, Y. Okada, J.M. Thomas, A.A. Genazzani, S. Patel, A. Galione, NAADP mobilizes Ca(2+) from reserve granules, lysosome-related organelles, in sea urchin eggs, Cell 111 (2002) 703–708.

[45] T. Pozzan, R. Rizzuto, P. Volpe, J. Meldolesi, Molecular and cellular physiology of intracellular calcium stores, Physiol. Rev. 74 (1994) 595–636.

[46] M.F. Langhorst, N. Schwarzmann, A.H. Guse, Ca2+ release via ryanodine receptors and Ca2+ entry: major mechanisms in NAADP-mediated Ca2+ signaling in T-lymphocytes, Cell. Signal. 16 (2004) 1283–1289.

[47] E. Brailoiu, J.L. Hoard, C.M. Filipeanu, G.C. Brailoiu, S.L. Dun, S. Patel, N.J. Dun, Nicotinic acid adenine dinucleotide phosphate potentiates neurite outgrowth, J. Biol. Chem. 280 (2005) 5646–5650.

[48] Z. Padamsey, L. McGuinness, S.J. Bardo, M. Reinhart, R. Tong, A. Hedegaard, M.L. Hart, N.J. Emptage, Activity-dependent exocytosis of lysosomes regulates the structural plasticity of dendritic spines, Neuron 93 (2017) 132–146.

[49] Y.V. Osipchuk, M. Wakui, D.I. Yule, D.V. Gallacher, O.H. Petersen, Cytoplasmic Ca2+ oscillations evoked by receptor stimulation, G-protein activation, internal application of inositol trisphosphate or Ca2+: simultaneous microfluorimetry and Ca2+ dependent Cl- current recording in single pancreatic acinar cells, EMBO J. 9 (1990) 697–704.

[50] P. Thorn, O. Gerasimenko, O.H. Petersen, Cyclic ADP-ribose regulation of ryanodine receptors involved in agonist evoked cytosolic Ca2+ oscillations in pancreatic acinar cells, EMBO J. 13 (1994) 2038–2043.

[51] J.M. Cancela, O.H. Petersen, The cyclic ADP ribose antagonist 8-NH2-cADP-ribose blocks cholecystokinin-evoked cytosolic Ca2+ spiking in pancreatic acinar cells, Pflugers Arch. 435 (1998) 746–748.

[52] H. Kasai, G.J. Augustine, Cytosolic Ca2+ gradients triggering unidirectional fluid secretion from exocrine pancreas, Nature 348 (1990) 735–738.
[53] A. Zdebik, M.J. Hug, R. Greger, Chloride channels in the luminal membrane of rat pancreatic acini, Pflugers Archiv: Eur. J. Physiol. 434 (1997) 188–194.
[54] J.E. Melvin, Chloride channels and salivary gland function, Crit. Rev. Oral Biol. Med. 10 (1999) 199–209.
[55] J.E. Melvin, D. Yule, T. Shuttleworth, T. Begenisich, Regulation of fluid and electrolyte secretion in salivary gland acinar cells, Annu. Rev. Physiol. 67 (2005) 445–469.
[56] H. Tsuboi, I. Matsumoto, E. Wakamatsu, Y. Nakamura, M. Iizuka, T. Hayashi, D. Goto, S. Ito, T. Sumida, New epitopes and function of anti-M3 muscarinic acetylcholine receptor antibodies in patients with Sjogren's syndrome, Clin. Exp. Immunol. 162 (2010) 53–61.
[57] S. Bacman, L. Sterin-Borda, J.J. Camusso, R. Arana, O. Hubscher, E. Borda, Circulating antibodies against rat parotid gland M3 muscarinic receptors in primary Sjogren's syndrome, Clin. Exp. Immunol. 104 (1996) 454–459.
[58] J. He, L. Qiang, Y. Ding, P. Wei, Y.N. Li, H. Hua, Z.G. Li, The role of muscarinic acetylcholine receptor type 3 polypeptide (M3RP205-220) antibody in the saliva of patients with primary Sjogren's syndrome, Clin. Exp. Rheumatol. 30 (2012) 322–326.
[59] L.Y. Teos, Y. Zhang, A.P. Cotrim, W. Swaim, J.H. Won, J. Ambrus, L. Shen, L. Bebris, M. Grisius, S.I. Jang, D.I. Yule, I.S. Ambudkar, I. Alevizos, IP3R deficit underlies loss of salivary fluid secretion in Sjogren's Syndrome, Sci. Rep. 5 (2015) 13953.